

Geographical CO₂ sensitivity of phytoplankton correlates with ocean buffer capacity

Running head: Phytoplankton response to ocean buffer capacity

Sophie Richier^{1*}, Eric. P. Achterberg^{1,2}, Matthew P. Humphreys^{1,3}, Alex J. Poulton^{4,5}, David J Suggett^{6,7}, Toby Tyrrell¹, C. Mark Moore¹

¹Ocean and Earth Science, National Oceanography Centre Southampton, University of Southampton, Southampton, UK

²GEOMAR Helmholtz Centre for Ocean Research, 24148 Kiel, Germany

³Centre for Ocean and Atmospheric Sciences, School of Environmental Sciences, University of East Anglia, Norwich, UK

⁴National Oceanography Centre, Southampton, UK

⁵Current address: The Lyell Centre, Heriot-Watt University, Edinburgh, UK

⁶School of Biological Sciences, University of Essex, Essex, UK

⁷Climate Change Cluster (C3), University of Technology Sydney, P.O. Box 123 Broadway, NSW 2007, Australia

Corresponding author*:

Dr Sophie Richier
University of Southampton,
National Oceanography Centre,
European Way, SO14 3ZH Southampton, UK
Email: sophie.richier@ceva.fr
Phone: +44 (0) 2380594801

Keywords: carbonate chemistry, carbonate system buffer capacity, anthropogenic

change, ocean acidification, cell size, experimental manipulation

Type of paper: Primary research

Abstract

Accumulation of anthropogenic CO₂ is significantly altering ocean chemistry. A range of biological impacts resulting from this oceanic CO₂ accumulation are emerging, however the mechanisms responsible for observed differential susceptibility between organisms and across environmental settings remain obscure. A primary consequence of increased oceanic CO₂ uptake is a decrease in the carbonate system buffer capacity, which characterises the system's chemical resilience to changes in CO₂, generating the potential for enhanced variability in *p*CO₂ and the concentration of carbonate [CO₃²⁻], bicarbonate [HCO₃⁻] and protons [H⁺] in the future ocean. We conducted a meta-analysis of 17 shipboard manipulation experiments performed across three distinct geographical regions that encompassed a wide range of environmental conditions from European temperate seas to Arctic and Southern oceans. These data demonstrated a correlation between the magnitude of natural phytoplankton community biological responses to short-term CO₂ changes and variability in the local buffer capacity across ocean basin scales. Specifically, short-term suppression of small phytoplankton (<10 µm) net growth rates were consistently observed under enhanced *p*CO₂ within experiments performed in regions with higher ambient buffer capacity. The results further highlight the relevance of phytoplankton cell size for the impacts of enhanced *p*CO₂ in both the modern and future ocean. Specifically, cell-size related acclimation and adaptation to regional environmental variability, as characterised by buffer capacity, likely influences interactions between primary producers and carbonate chemistry over a range of spatio-temporal scales.

Introduction

Phytoplankton play a pivotal role in marine ecosystems and ocean biogeochemistry, and hence have been the focus of intensive research into the potential for ongoing changes in marine carbonate chemistry driven by the continued uptake of anthropogenic atmospheric CO₂ (often termed ocean acidification, OA) (Royal Society, 2005; Doney *et al.*, 2009) to influence their physiology, ecology and productivity. Phytoplankton have been demonstrated to display a variety of physiological sensitivities to OA within experimental manipulations performed over a range of timescales (Riebesell & Tortell, 2011; Kroeker *et al.*, 2013; Collins *et al.*, 2014; Wu *et al.*, 2014; Dutkeiwicz *et al.*, 2015; Riebesell *et al.*, 2017). However, robust reproducible responses and a clear mechanistic understanding of the observed differential responses have remained elusive (Kroeker *et al.*, 2013; Flynn *et al.*, 2012; Bach *et al.*, 2015).

In addition to altering the absolute concentrations of a range of chemical species, including $p\text{CO}_2$, carbonate [CO₃²⁻], bicarbonate [HCO₃⁻] and protons [H⁺], OA also leads to decreases in the carbonate system buffer capacity (Eggleston *et al.*, 2010; Frankignoulle, 1994). Carbonate chemistry system (CCS) variability as a result of both biotic and abiotic forcing is thus expected to increase in the future ocean (Flynn *et al.*, 2012; Eggleston *et al.*, 2010). Moreover, these ongoing changes in carbonate chemistry are occurring against a background of both natural and anthropogenically altered gradients in a range of other potentially interacting environmental drivers of phytoplankton ecophysiology (Boyd *et al.*, 2010, 2015; 2016), including temperature (Kroeker *et al.*, 2013; Tatters *et al.*, 2013; Humphreys, 2017) and nutrient availability (Hoppe *et al.*, 2013; Muller *et al.*, 2017). Integrative understanding of how OA is likely to influence phytoplankton ecophysiology, and consequently ocean biogeochemistry, requires an appreciation of the potential for variability in a range of these environmental conditions to modulate responses (Boyd, 2011).

Within experimental studies, significant physiological responses to altered carbonate chemistry for any given organism might be expected under those conditions where the magnitude and/or frequency of any imposed change exceeds that of current acclimative tolerance (Joint *et al.*, 2011; Denman *et al.*, 2011; Lewis *et al.*, 2013; Richier *et al.*, 2014; Boyd *et al.*, 2016). In addition to dictating the response to experimental manipulation (Richier *et al.*, 2014), differential acclimative potential across organisms may also influence the emergent outcome of community responses to the longer-term environmental perturbation represented by OA (Lohbeck *et al.*, 2012; Reusch & Boyd, 2013; Schaum *et al.*, 2013, 2016; Hendricks *et al.* 2015). Indeed, differential sensitivity to dynamic changes in carbonate chemistry might be expected on the basis of theoretical considerations (Flynn *et al.*, 2012) and has recently been demonstrated for phytoplankton, specifically between coastal and open ocean diatom taxa (Li *et al.*, 2016).

Understanding the fundamental controls on acclimative tolerance to carbonate chemistry variability and adaptive differences in such tolerances between groups and across environmental gradients is essential for predicting natural phytoplankton community responses to OA-type perturbations over space and time (Flynn *et al.*, 2012, 2015; Lewis *et al.*, 2013; Schaum *et al.*, 2016; Li *et al.*, 2016). We therefore investigated whether differential responses in the sensitivity of phytoplankton to short-term changes in the CCS were observable within natural communities, and whether such variability related to ocean scale gradients in environmental conditions. Using a unique data set of 17 mesocosm experiments spanning 7 regional seas (i.e. from the Greenland to the Weddell seas) and 3 ocean regions (from the Arctic to the Southern oceans), we relate observable differential biological responses to the susceptibility of the local system to dynamic changes in carbonate chemistry variables, as quantified by the buffer capacity, while investigating other potentially confounding factors including nutrient availability.

Materials and Methods

Seawater collection and experimental set up

A series of 17 shipboard multi-treatment manipulation experiments were conducted using equivalent protocols on three cruises (Fig. 1). The first cruise (D366) took place in northwest European shelf seas during summer on the RRS *Discovery* (2011 June 6-July 12) (Richier *et al.*, 2014). Two subsequent cruises (JR271 and JR274 respectively) were carried out in the Arctic (2012 June 1- July 2) (Poulton *et al.*, 2016) and Southern (2013 January 9-February 12) (Tarling *et al.*, 2016) oceans, both on board the RRS *James Clark Ross*.

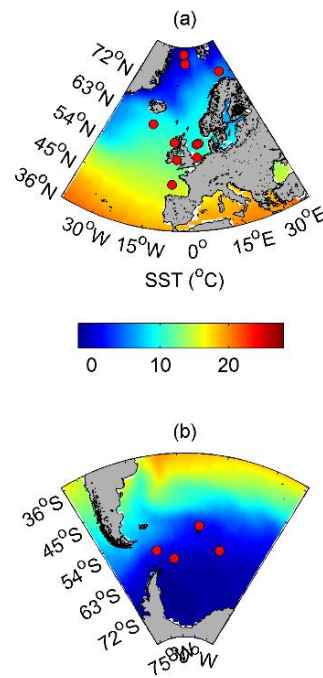


Figure 1. Locations of experiments throughout the three cruises. Sea surface temperature (SST; °C) varied markedly across experimental locations (a, b). Red dots illustrate experimental locations.

118 Locations, oceanographic settings and treatments applied within each experiment are
 119 presented in Tables 1 and 2.

120

Cruise	Exp.	Variables manipulated	Conditions	Incubation duration (days)	Sampling-points (days)
D366	1	Carbonate chemistry	$p\text{CO}_2$ [550, 750 and 1000 μatm]	4	0, 2, 4
	2	Carbonate chemistry	$p\text{CO}_2$ [550, 750 and 1000 μatm]	4	0, 2, 4
	2b	Carbonate chemistry + nutrients	$p\text{CO}_2$ [750 μatm] ; nutrients [+N, +P, +NP]*	2	0, 2
	3	Carbonate chemistry	$p\text{CO}_2$ [550, 750 and 1000 μatm]	4	0, 2, 4
	4	Carbonate chemistry	$p\text{CO}_2$ [550, 750 and 1000 μatm]	4	0, 2, 4
	4b	Carbonate chemistry + nutrients	$p\text{CO}_2$ [750 μatm] ; nutrients [+N, +P, +NP]*	2	0, 2
	5	Carbonate chemistry	$p\text{CO}_2$ [550, 750 and 1000 μatm]	4	0, 2, 4
	5b	Carbonate chemistry + nutrients	$p\text{CO}_2$ [750 μatm] ; nutrients [+N, +P, +NP]*	2	0, 2
JR271	1-5	Carbonate chemistry	$p\text{CO}_2$ [550, 750 and 1000 μatm]	4	0, 2, 4
JR274	1	Carbonate chemistry + nutrients	$p\text{CO}_2$ [750 μatm] ; nutrients [+Fe]*	4	0, 2, 4
	2	Carbonate chemistry + nutrients	$p\text{CO}_2$ [750 μatm] ; nutrients [+Fe]*	6	0, 3, 6
	3	Carbonate chemistry	$p\text{CO}_2$ [750, 1000 and 2000 μatm]	6	0, 3, 6
	4	Carbonate chemistry	$p\text{CO}_2$ [750, 1000 and 2000 μatm]	8	0, 4, 8

121

122 **Table 1: Bioassay experiment set up conditions.** Concentration of nutrients* added to the
 123 incubation bottles were the following: +N: 2 $\mu\text{mol L}^{-1}$, +P: 0.2 $\mu\text{mol L}^{-1}$, +Si: 2 $\mu\text{mol L}^{-1}$,
 124 +Fe: 2 nmol L^{-1} .

125

126

Cruise	Exp.	Date	Lat. (°N/S)	Long. (°W/E)	DIC ($\mu\text{mol. kg}^{-1}$)	TA ($\mu\text{mol. kg}^{-1}$)	SST (°C)	Salinity	Depth (m)	NO ₃ ⁻ ($\mu\text{mol. L}^{-1}$)	PO ₄ ³⁻ ($\mu\text{mol. L}^{-1}$)	Si(OH) ₄ ($\mu\text{mol. L}^{-1}$)	Chl- <i>a</i> ($\mu\text{g. L}^{-1}$)
D366	1	8.06.11	56 47.27 N	7 25.01 W	2091.8 (0.9)	2310.9 (2.3)	11.27	34.8	6	1.1 (0.1)	0.1 (0.0)	2.1 (0.2)	3.2(0.0)
	2	14.06.11	52 28.23 N	5 54.05 W	2094.5 (0.9)	2322.2 (2.4)	11.77	34.44	5	0.3 (0.0)	0.1 (0.0)	0.4 (0.0)	3.5 (0.1)
	2b	19.06.11	46 29.70 N	7 12.67 W	2085.8	2345.6	15.02	37.67	<10	0.9 (0.1)	0.1 (0.0)	1.1 (0.0)	0.5 (0.0)
	3	21.06.11	46 12.14 N	7 13.25 W	2083.8 (0.6)	2347.1 (3.6)	15.31	35.77	10	0.6 (0.0)	0.1 (0.0)	0.6 (0.0)	0.8 (0.0)
	4	26.06.11	52 59.66 N	2 29.84 E	2085.5 (1.6)	2295.6 (0.4)	14.57	34.05	5	0.9 (0.1)	0.1 (0.0)	0.8 (0.0)	1.3 (0.0)
	4b	29.06.11	57 45.93 N	4 35.26 E	2053.2	2291.9	13.09	34.80	<10	0.3	0.0	0.3	0.5 (0.0)
	5	02.07.11	56 30.29 N	3 39.51 E	2084.6 (1.5)	2310.8 (3.2)	13.86	34.99	12	0.3 (0.2)	0.1 (0.0)	0.1 (0.0)	0.2 (0.2)
	5b	03.07.11	59 40.67 N	4 06.92 E	1997.2	2214.0	13.30	30.50	<10	0.3 (0.0)	0.0	0.0	0.8 (0.0)
JR271	1	03.06.12	56 16.00 N	2 37.99 E	2082.3 (0.5)	2325.3 (0.4)	10.78	35.12	10	0.0 (0.0)	0.1 (0.0)	1.3 (0.0)	0.3 (0.0)
	2	08.06.12	60 35.62 N	18 51.39 W	2086.8 (1.0)	2323.4 (2.4)	10.65	35.25	21	5.0 (0.1)	0.3 (0.0)	1.6 (0.2)	1.8 (0.3)
	3	13.06.12	76 10.51 N	2 32.96 W	2130.0 (3.2)	2305.3 (6.5)	1.67	34.93	18	9.2 (0.0)	0.65 (0.0)	5.8 (0.0)	0.9 (0.0)
	4	18.06.12	78 21.15 N	3 39.85 W	2106.4 (5.7)	2234.6 (2.9)	-1.6	32.59	7	4.2 (0.1)	0.79 (0.0)	12.21 (0.0)	3.0 (0.3)
	5	24.06.12	72 53.49 N	26 00.20 E	2108.7 (2.0)	2314.0 (4.0)	6.55	34.97	10	5.38 (0.5)	0.4 (0.0)	3.9 (0.1)	1.2 (0.2)
JR274	1	13.01.13	58 22.00 S	56 15.12 W	2129.8 (1.1)	2293.2 (0.8)	1.94	33.90	33	22.7 (0.1)	1.3 (0.0)	15.5 (0.1)	2.3 (0.1)
	2	18.01.13	61 04.70 S	48 21.58 W	2145.2 (0.1)	2281	-1.44	33.58	19	25.5 (0.2)	1.7 (0.0)	63.5 (0.4)	0.5 (0.1)
	3	25.01.13	52 41.36 S	36 37.28 W	2152.3 (6.1)	2287.8	2.17	33.94	26	24.4 (0.2)	1.6 (0.0)	18.1 (0.1)	0.6 (0.1)
	4	01.02.13	58 05.13 S	25 55.55 W	2129.5 (4.3)	2293	0.51	33.70	19	18.9 (0.6)	1.2 (0.0)	72.4 (0.5)	4.2 (0.4)

127

128 **Table 2. Initial conditions (average \pm SD) for the bioassay experiments set up along three**
129 **crises.** Salinity, depth and sea surface temperature (SST) were measured *in situ* using the CTD
130 sensor.
131

132 Specific cleaning and handling techniques were followed during setup of each of the
133 experiments. Briefly, the incubation bottles (Polycarbonate, Nalgene™) were acid-cleaned in
134 1% HCl followed by three de-ionised water (Milli-Q, Millipore) rinses during the low-latitude
135 cruise (D366). Further extensive cleaning procedures were applied during cruises in
136 potentially iron-limited regions of the ocean (i.e. high-latitude regions; Figs. 1a and b).
137 Bottles, upon first use, were filled up to the neck with detergent (1% Decon) for 1 day
138 followed by three rinses with de-ionised water, and then filled with 10% HCl (Aristar grade)
139 for 3 days followed by three rinses with de-ionised water.

On the day of the experimental setup, vertical profiles of temperature, salinity, oxygen, chlorophyll fluorescence, turbidity and Photosynthetically Active Radiation (PAR) were obtained in order to select and characterise the depth of experimental water collection within the wider water column (Richier *et al.*, 2014). Unfiltered near-surface (≤ 33 m) seawater containing the extant natural microbial community was collected at the different stations using Niskin bottles attached to a CTD rosette. The total of up to 480 L of seawater required for each experiment was collected using 24×20 L OTE (Ocean Test Equipment) bottles and dispensed from randomly assigned OTE bottles through silicon tubing amongst 4.5 L (all experiments) or 1.25 L (experiments 2b, 4b and 5b during D366) polycarbonate bottles.

Multi-treatment (≥ 4 conditions; Table 1) manipulation experiments were incubated in a purposely-converted commercial refrigeration container located on the aft deck of the ship. Temperature was maintained ($\pm < 1$ °C) at the *in situ* value at the time of water collection (Table 2). Irradiance ($100 \mu\text{mol quanta m}^{-2} \text{ s}^{-2}$) was provided by daylight simulation LED panels (Powerpax, UK) over a light-dark cycle approximating the ambient photoperiod: 18-6 h light-dark (D366 and JR274) or 24 h continuous light (JR271, except for experiment E1 with 18-6 h).

The majority of experiments (14 out of 17) were run for ≥ 4 days and involved 2 sampling points following measurement of initial conditions. Independent incubation bottles were sacrificed at every sampling point (Table 1). Specifically, the majority of the experiments (11 out of 17) were run using identical durations with sampling points at 0, 2 and 4 days and almost all (14 out of 17) included a time point measured after 2 days of incubation, with the shortest resolved timescales often corresponding to the most marked observed biological responses (Richier *et al.*, 2014). The 3 experiments including inorganic nutrient addition (E2b, E4b and E5b) during the first cruise (D366) were run under the same temperature and light regime for a shorter incubation period of 2 days with a single sampling

point at the end, corresponding to the timescale over which maximum response effects were observed during this cruise (Richier *et al.*, 2014).

Following the failure to observe strong responses within those experiments performed in higher latitude low temperature systems during the second cruise (JR271; Poulton *et al.*, 2016), we subsequently increased incubation timescales for a subset number of experiments on the final cruise (JR274) (Table 1). Specifically, the potential for the observed continued lack of strong responses to be related to slower microbial metabolism within the low temperature waters encountered was investigated by running 3 experiments of increasingly longer total duration from 4 to 6 to 8 days, and through the inclusion of a higher target $p\text{CO}_2$ condition of 2000 μatm (Table 1). Subsequently, response magnitudes were found to be independent of overall experimental duration (see below).

Variables measured

Total and size fractionated chlorophyll

Total community chlorophyll concentrations were measured according to the method described in Richier *et al.* (2014). Briefly, aliquots of 100 mL were sampled from every incubation bottle and filtered onto 25 mm GF/F filters (Whatman, 0.7 μm nominal pore size) or 10 μm pore size polycarbonate filters (Whatman) (to yield a total and a $> 10 \mu\text{m}$ size fraction, respectively and therefore by difference a $< 10 \mu\text{m}$ size fraction). Filters were extracted into 6 mL 90% HPLC-grade acetone overnight at 4 °C in the dark and fluorescence was then measured using a fluorometer (Turner Designs Trilogy) following Welschmeyer (1994).

Variable chlorophyll fluorescence (F_v/F_m)

The photosynthetic physiology of total communities was measured according to the method described in Richier *et al.* (2014) on a Chelsea Scientific Instruments FastTracka II™ Fast Repetition Rate fluorometer (FRRf). Briefly, all samples were dark acclimated for 30 min and FRRf measurements were corrected for the blank effect using carefully prepared 0.2 µm filtrates for all experiments and time points (Cullen & Davis, 2003). F_v/F_m was taken as an estimate of the apparent photosystem II photochemical quantum efficiency (Kolber *et al.*, 1998).

Particulate organic matter

Measurements of particulate organic carbon, nitrogen and phosphorous (POC, PON and POP, respectively) were used as indices of relative changes in overall microbial community biomass, noting that detrital material can form a significant component of all of these pools. Although ratios of POC:PON:POP varied across the entire data set (not shown), treatment specific patterns of variability in all these particulate organic matter pools generally co-varied (Richier *et al.*, 2014). Consequently, here we only present the most complete data set (POP), noting that conclusions would not differ if using POC or PON, but would be based on a more limited subset of experiments.

Measurements of POP were performed as previously described (Richier *et al.*, 2014). Aliquots of 750 mL of seawater were filtered onto 25 mm glass fibre filters (Fisher MF 300, effective pore size 0.7 µm), which had been pre-combusted at 400 °C, soaked in 10 % HCl for 24 h and rinsed in two subsequent de-ionised water baths for 12 h each. Following filtration, each filter was oven-dried at 60 °C for 8 to 12 h and POP content was measured according to the method described in Raimbault *et al.* (1999). Briefly, POP compounds were converted into inorganic products by a persulfate wet-oxidation under slightly alkaline conditions. After

oxidation, inorganic products were dissolved in a digestion mixture, autoclaved and analysed for phosphate in a Segmented Flow Auto Analyser. In order to estimate the oxidation efficiency of the method, standard organic compounds (Standard reference Material® 1573a) were used.

Overall, up to 39 variables (biological, chemical and physical) were measured in each of the 17 experiments run during the three cruises (results not shown). Sample treatments and analyses followed the methods described in Richier *et al.* (2014).

Carbonate chemistry manipulation

Sampling was performed on deck for the D366 cruise and inside a trace-metal-clean container for the two polar cruises (JR271 and JR274).

Subsamples for carbonate chemistry analyses were taken from the CTD at time zero (t_0), and TA and DIC were immediately measured using a TA Titrator (AS-ALK2) and a DIC Analyzer (AS-C3) (Apollo SciTech), respectively. The results were calibrated using measurements of certified reference material obtained from A.G. Dickson (Scripps Institution of Oceanography, USA). The remaining CCS variables were calculated with the CO₂SYS programme (version 1.05) (Lewis & Wallace, 1998; Pierrot *et al.*, 2006) run in a MATLAB™ environment and using the carbonic acid dissociation constants of Mehrbach *et al.* (1973) refitted by Dickson & Millero (1987). The 1σ precisions for DIC and TA measurements were estimated as ± 3.8 and ± 2.0 $\mu\text{mol kg}^{-1}$ respectively (Tynan *et al.*, 2016).

DIC and TA were subsequently measured on a separate set of manipulated reference bottles at t_0 , as well as within all subsequently sampled time point bottles. This checked the performance of the manipulation method, as well as monitored the magnitude of any changes in carbonate chemistry due to ongoing biological activity within the incubation bottles over

the experimental duration (Richier *et al.*, 2014; Riebesell & Tortell, 2011). Such changes are presented in Figure S2 with measured $p\text{CO}_2$ typically within 25% of target values at the first time point, while biological activity had generated differences of over 50% from target by the final time points.

Incubation bottles were filled without headspace and immediately manipulated using an equimolar addition of strong acid (1 M HCl) and HCO_3^- (1 M) (Richier *et al.*, 2014). In the case of the polar cruises, trace metal clean HCl (Romil, UHP) was used, and all reagents were pre-cleaned using a Chelex® cation chelation column (Sunda *et al.*, 2005). Within a subset of the experiments, inorganic nutrients were also manipulated through addition of major macronutrients (nitrate (NO_3^-), silicic acid (dSi) and phosphate (PO_4^{3-})) or a trace nutrient (DFe) in a factorial manner under both the ambient state of the carbonate system or in addition to being manipulated towards a target $p\text{CO}_2$ (Table 1).

Biological replicates and statistical power

Bioassay experiments were set up with seawater collected from either one (D366) or three (JR271 and JR274) dedicated CTDs deployed successively. Independent biological replication, corresponding to a minimum of triplicates per experimental treatment, was maintained subsequent to the initial point of sampling, which corresponded to the closure of a given OTE bottle within the sampled water column, with triplicates during JR271 and JR274 being taken from independent CTD casts. To provide for robust statistical testing of treatment effects alongside sufficient water to perform all required analyses, 9 bottles were used for each of the 4 treatments in 3 sets of triplicates (see Richier *et al.* (2014) for further details). Subsamples ($n = 3$) were collected simultaneously for t_0 measurements of each of the variables to be measured over the subsequent time course (Table 1).

Data normalisation and statistical analysis

Experimental time courses of biomass and other variable changes were often complex (see below). In order to produce a method of combining data across multiple cruises / environments, individual response variables (e.g. Chl, POP, F_v/F_m) measured across the experimental treatments (i.e. across the range of target $p\text{CO}_2$ levels) were normalised to values measured in control bottles at the same time point. This allows us to derive a normalised effect magnitude for every time point, treatment and variable, i.e. for every variable and treatment:

$$(1) \text{Var}_{\text{effect, treatment}} = (\text{Var}_{\text{Treatment}} - \text{Var}_{\text{Control}}) / \text{Var}_{\text{Control}}$$

For example, the magnitude of the 750 μatm target $p\text{CO}_2$ treatment effect for Chl within an experiment was given by:

$$(2) \text{Chl}_{\text{effect, 750}} = (\text{Chl}_{750} - \text{Chl}_{\text{Control}}) / \text{Chl}_{\text{Control}}$$

yielding a normalised treatment variable which is equivalent to the net integrated difference in the total community Chl growth rate between the control and the stated (in this case 750 μatm $p\text{CO}_2$) treatment. As a result of differences in sampled time points for some experiments (Table 1) and variability in the magnitude of the treatment effect over time within experiments displaying strong responses (Richier *et al.*, 2014), we also compared maximum differential sensitivities of biological responses to CCS manipulation across the full suite of experiments. Here we chose the maximum values of the normalised treatment effect over the experimental duration so that the maximal normalised treatment effects (MNTE) represented the maximum observed differential response between a treatment and the control condition over all sampling time points for any given treatment in any given experiment. As discussed elsewhere, the strongest MNTEs were typically observed at the shortest timescales (2 day) resolved (Richier *et al.*, 2014).

Tests for statistical differences ($p < 0.05$) between all treatments and controls were subsequently performed within all individual experiments using 1-way ANOVA followed by Tukey-Kramer means comparison tests. For simplicity, here we only quote significant differences between controls and treatments, noting that significant increases in treatment effect as a function of imposed CCS manipulation did occur (Richier et al. 2014). Subsequently, statistically significant correlations ($p < 0.05$, $n = 17$) between the magnitude of treatment effects, as determined by the normalized observed difference between the control treatment and the 750 μatm treatment(s) (i.e. MNT_{750}) observed across all experiments, and the range of measured initial conditions across all the experiments were assessed using Pearson's product-moment correlation.

Results

Variability in responses across environmental settings

Incubation of natural samples alongside manipulations of the carbonate chemistry system (CCS) and nutrients (Table 1) produced complex time-varying responses in many of the performed experiments (Fig. 2), likely reflecting the range of different environmental conditions (Table 2) and associated community structures encountered across the full suite of experiments. Overall biomass was observed to increase (e.g. Fig. 2a, h, i), remain relatively constant (e.g. Fig. 2b, d), or occasionally decline within certain treatments (e.g. Fig. 2d, f). Moreover, although addition of the limiting nutrient(s), macronutrients nitrogen (N) and phosphorous (P) for D366 (Richier *et al.*, 2014) and iron (Fe) for JR274 (Fig. 2g) invariably resulted in a divergence between treatments, differential treatment effects were only observed as a function of CCS manipulation in a subset of the experiments (e.g. Fig. 2d-f). In order to

reduce the data and investigate the potential drivers of this observed differential sensitivity to CCS manipulation, we thus calculated MNTEs as described above.

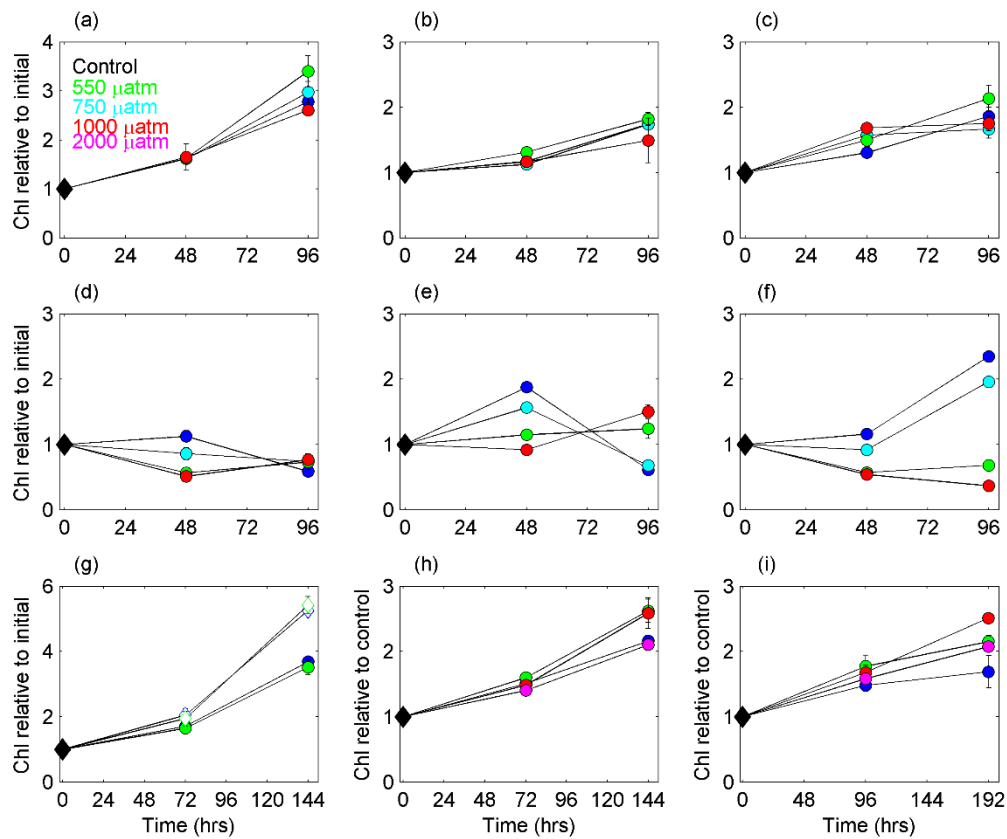


Figure 2. Time series measurements of total Chl *a* normalized to initial condition [see equations 1 & 2] for 9 representative examples from the 17 experiments. Examples plotted are from the Arctic, cruise JR271 experiments 3 (a), 4 (b) and 5 (c), the temperate waters of the European continental shelf, cruise D366 experiments 3 (d), 4 (e) and 5 (f) and the Southern Ocean, cruise JR274, experiments 2 (g), 3 (h), 4 (i). Plotted values are means ± 1 SE, for biological triplicates, with colours indicating experimental treatment as labelled in (a). Note, open symbols in (g) indicate treatments amended with Fe.

Relative responses of microbial communities against latitude

In total, across our full suite of experiments and target $p\text{CO}_2$ levels, up to 48 comparisons between triplicate sets of biological treatments and control bottles were possible, with statistically significant CCS treatment effects expressed as MNTes observable in around 30% of the comparisons (Figs. 3 and 4).

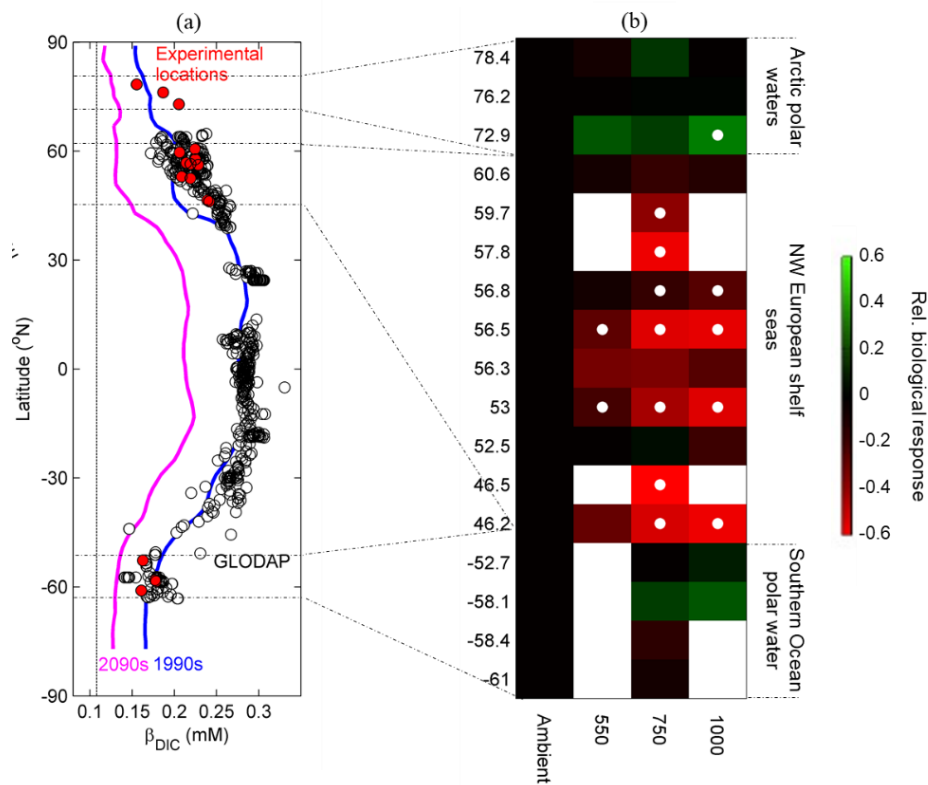


Figure 3. Latitudinal gradients in natural buffer factor and relative responses of microbial communities against latitude. Marked natural gradients in the H^+ buffer factor (β_{DIC}) are present in the Atlantic Ocean and were sampled across the full suite of experiments (a). Maximum values of biological responses normalised to controls observed over the duration of each experiment [see equation (2)] presented as a function of treatment and latitude, with the colour scale on the right side indicating the magnitude of response (b). Observed natural large scale oceanic gradients in *in situ* buffer factors (a) were derived from the Global Ocean Data Analysis Project (GLODAP) database (Key *et al.* 2004) with

comparative modelled environmental gradients for the 1990s-2090s (dark blue and pink lines, respectively) (Yool *et al.*, 2013). Vertical dotted line in (a) indicates the approximate minimum buffer factors expected as DIC approaches TA (Egleston *et al.*, 2010). Significant differences between treatments and controls in (b) are indicated by white dots (ANOVA, Tukey-Kramer, $p < 0.05$, $N = 3$).

As previously reported (Richier *et al.*, 2014), experiments performed at mid-latitudes (Fig. 3) consistently revealed relative decreases in net growth, as indicated by total chlorophyll (Chl) accumulation (Fig. 3), phytoplankton cell counts (Richier *et al.*, 2014) and indices of overall community biomass (Fig. 4), under enhanced $p\text{CO}_2$ (and hence changes in other CCS variables, such as $[\text{H}^+]$). In contrast, the apparent photosynthetic efficiency of phytoplankton communities was less affected (Fig. 5).

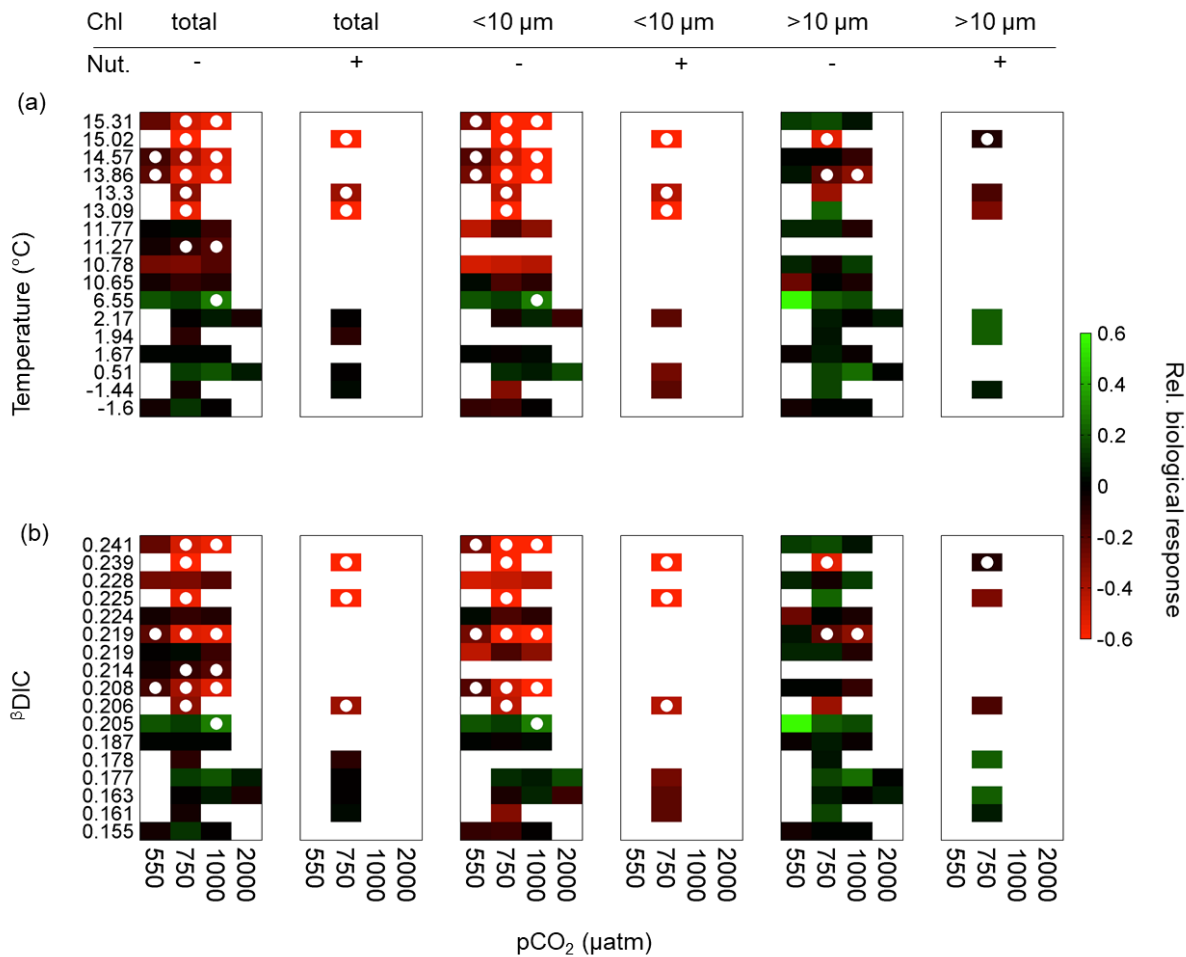


Figure 4. Ranked relative biological responses of natural microbial communities to altered $p\text{CO}_2$. Observed maximum values of control normalised experimental responses to increased $p\text{CO}_2$ across all 17 natural microbial communities analysed. Phytoplankton responses are presented for total and size fractionated ($<10\ \mu\text{m}$ or $>10\ \mu\text{m}$) Chl across all measured target $p\text{CO}_2$ concentrations under experimental conditions with ('-') or without ('+') additional nutrient (Nut.) amendment. Experimental results were ranked in order of (a) ambient sea surface temperature (SST, $^{\circ}\text{C}$) or (b) initial H^+ buffer factor (β_{DIC}). Calculations, colour scales and statistical tests are as described for Fig. 3b.

Where statistically significant responses in total community Chl (Figs. 3) and microbial biomass accumulation were observed (Fig. 4), these effects scaled with the magnitude of the imposed shift in the CCS, with a progressive response such that $\text{MNTE}_{1000} > \text{MNTE}_{750} > \text{MNTE}_{550}$ (Fig. 3 and 4). In contrast, no statistically significant responses could typically be detected within identical experiments performed in the Southern Ocean, higher latitude North Atlantic and Arctic Oceans (Fig. 3), indicating a prevailing tolerance of polar ocean natural microbial populations to the imposed extreme and rapid changes to the CCS.

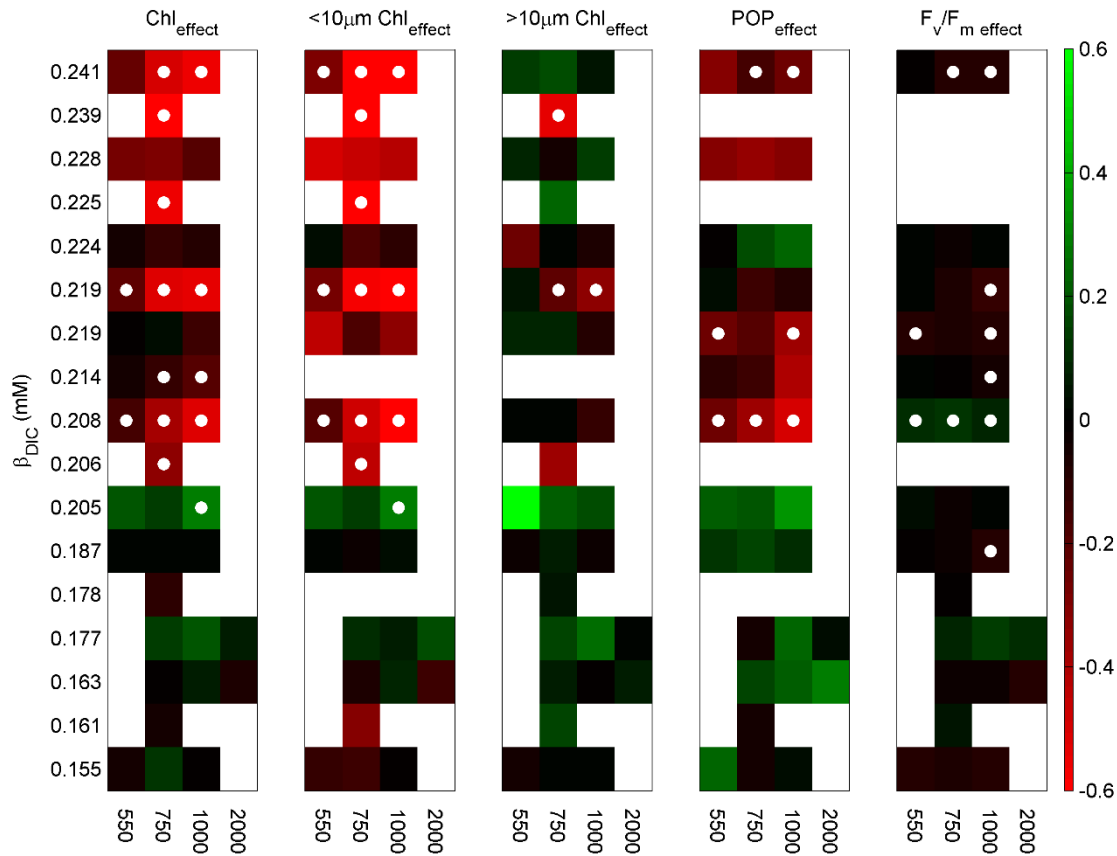


Figure 5. Response magnitudes of different variables ordered as a function of initial H^+ buffer factor (β_{DIC}). Colour scale on the right side indicates the magnitude of response with abbreviations, calculations and significant differences between treatments all as described for Figs. 3 & 4.

Drivers for the variable physiological susceptibility across phytoplankton communities

In order to identify potential environmental drivers for the marked variability in the biological responses to CCS manipulation we observed, we considered MNTes across all 17 experiments and manipulated pCO_2 levels (Figs. 3 and 4). In addition to scaling with the magnitude of the imposed experimental manipulation (targeted pCO_2 levels), the observed systematic differences in net total community Chl also scaled with increasing sea surface temperature (SST) and the correlated increases in buffer capacity (Sundquist *et al.*, 1979), as

quantified by the H^+ buffer factor ($\beta_{DIC} = (\partial \ln[H^+]/\partial DIC)^{-1}$) (Fig. 4; see Supplementary Information) (Egleston *et al.*, 2010).

The increased phytoplankton sensitivity to pCO_2 (and/or $[H^+]$ or other CCS variables) observed under warmer temperatures and higher buffer capacity conditions strongly correlated with, and was dominated by, the response (decreased net growth) of the smaller ($<10 \mu m$) size classes (Figs. 4 and S1). These coherent responses occurred irrespective of initial nutrient concentrations, which varied considerably between experiments (Table 2). Moreover, whilst parallel macronutrient and Fe additions (Table 1) enhanced net phytoplankton growth in the European shelf seas and Southern Ocean respectively, short-term responses to increasing pCO_2 were also observed irrespective of nutrient addition in the latter (Fig. 4). The overall MNTTE to CCS manipulation within these temperate ($>12^\circ C$) high-buffer capacity waters was of comparable magnitude to the nutrient MNTTEs (Fig. 6).

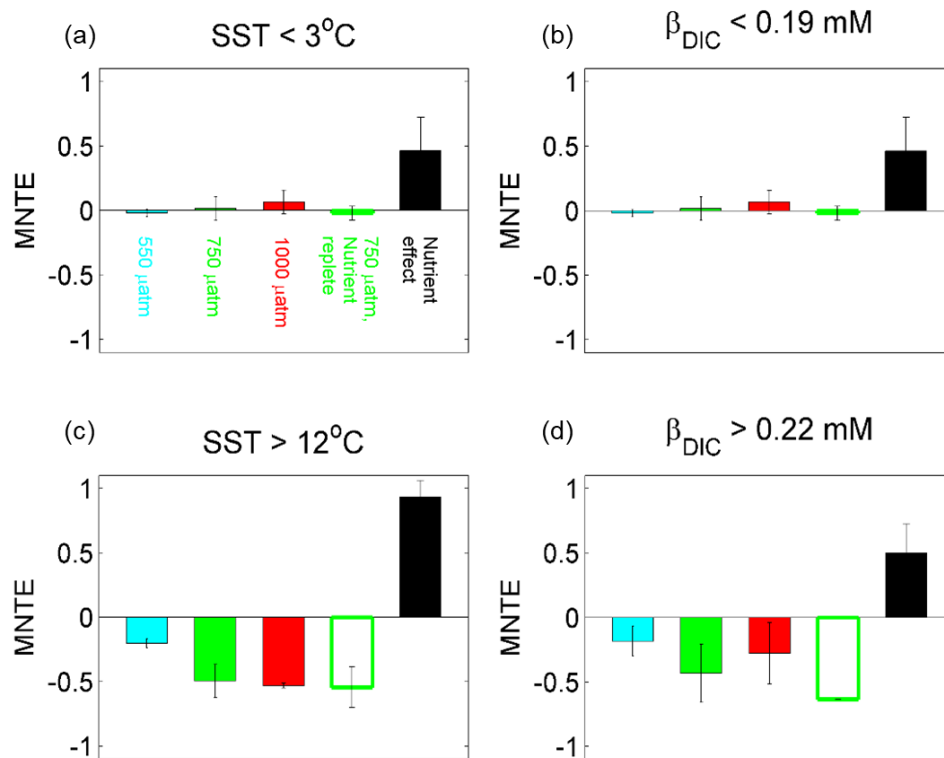
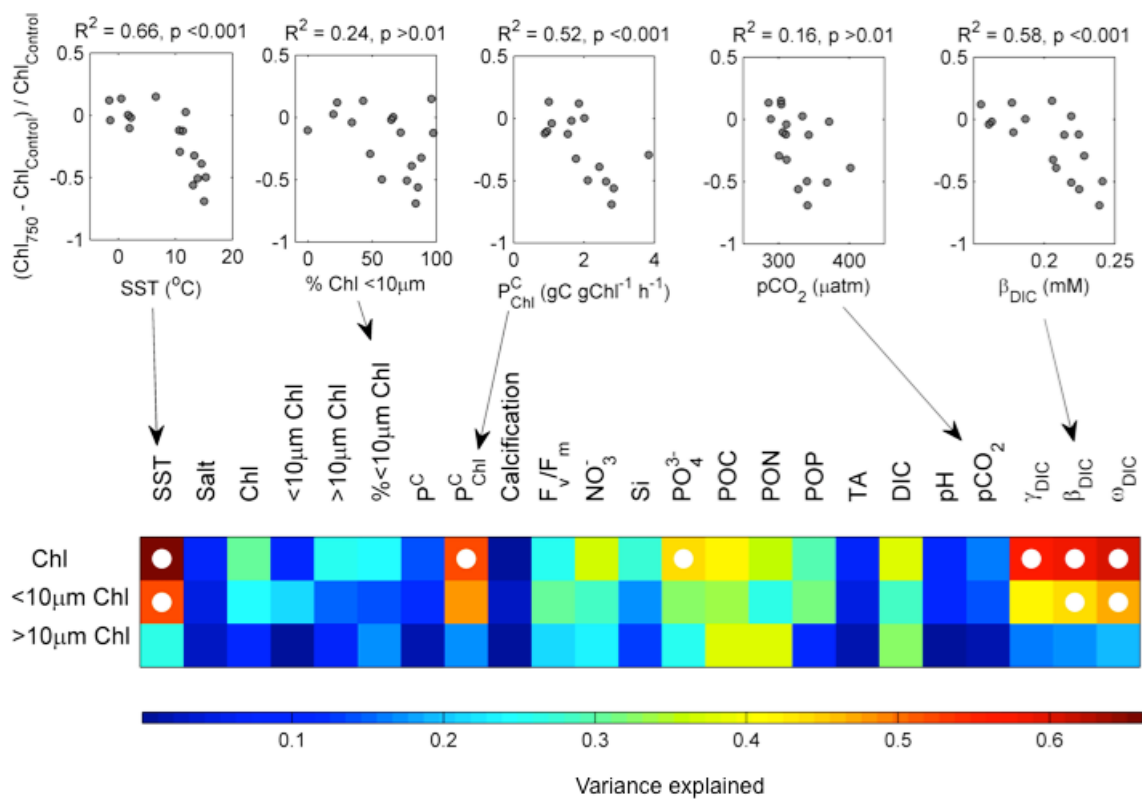


Figure 6. Maximal normalised treatment effects (MNTE) to variations in chemical species and nutrient addition. Maximal effects in response to $p\text{CO}_2$ (and hence $[\text{H}^+]$ etc.) manipulation and nutrient addition across all experiments grouped as (a, c) a function of temperature ($^{\circ}\text{C}$) and (b, d) initial H^+ buffer capacity (β_{DIC}). Plotted values are means ± 1 S.E. of the mean normalised responses across all experiments.

Observed responses within our $750 \mu\text{atm } p\text{CO}_2$ treatments (MNTE_{750}) were subsequently compared to a range of initial environmental conditions across all experiments (Fig. 7). Decreased net growth rates for bulk community and small sized phytoplankton ($<10 \mu\text{m}$) were significantly correlated with SST and CCS buffer factors (Fig. 7), statistically confirming the patterns observed across the full experimental/treatment data set (Fig. 4). Significant correlations were also observed between the bulk phytoplankton responses and both ambient phosphate concentrations and Chl-normalized photosynthetic rates (Fig. 7), which also tend to correlate with SST over large oceanic scales (Sundquist *et al.*, 1979; Behrenfeld & Falkowski, 1997). In contrast, differences in net phytoplankton growth rates as a function of imposed treatment displayed no correlation with any of the other wide range of initial physical, chemical and biological variables tested, including indices of initial community size structure (Fig. 7).



417 **Figure 7. Correlation between indices of normalised phytoplankton responses under the**
418 **750 μatm $p\text{CO}_2$ treatment and representative initial conditions.** Scatter plots of whole
419 community (total Chl) normalised phytoplankton responses in the 750 μatm treatment are
420 presented against representative initial conditions (top), alongside a heat map of correlation
421 coefficients between three indices of phytoplankton responses in the 750 μatm treatment and
422 the complete set of available initial conditions. The following abbreviations are used: sea
423 surface temperature (SST); Chlorophyll (Chl); photosynthetic rate (P^C); Chl normalized
424 photosynthetic rate (P^C_{Chl}); apparent photochemical quantum efficiency (F_v/F_m); particulate
425 organic carbon (POC); particulate organic nitrogen (PON); particulate organic phosphorous
426 (POP); total alkalinity (TA); dissolved inorganic carbon (DIC); $[\text{CO}_2]$, $[\text{H}^+]$ and carbonate
427 saturation state (Ω) buffer factors (γ_{DIC} , β_{DIC} and ω_{DIC} respectively, see Supplementary
428 information for details on buffer factors calculation). Correlation analyses between initial
429 conditions and the presented responses [total and size fractionated (<10 μm and >10 μm Chl)]

were performed across all 17 experiments with data normalised to the control treatment as described in Fig. 3b. White dots indicate significant correlations between responses and initial conditions ($p < 0.01$).

Discussion

Combined analysis of a large suite of experiments performed using near-identical protocols on multiple cruises across oceanic scales (Fig. 1), revealed differential biological responses which could be related to geographical ambient environmental conditions (Figs. 4 and 7). Specifically, the magnitude of observed biological responses to CCS manipulation varied as a function of latitude (Fig. 3), in association with correlated variability in ambient nutrient concentration (phosphate), temperature and CCS buffer capacity (Fig. 7). Organism responses to environmental forcing may vary as a function of interactions between any one or more such environmental drivers (Boyd *et al.*, 2010; 2016). For example, responses to CCS manipulation may vary as a function of nutrient availability (Li *et al.*, 2012; Richier *et al.*, 2014; Trimborn *et al.*, 2017), while temperature will also directly influence metabolic rates and potentially interact with variability in the CCS to determine organism responses (Flynn *et al.*, 2012; Humphreys, 2017).

In terms of nutrient availability, although MNTes correlated with phosphate availability (Fig. 7), this was unlikely to be causative. Similar responses could be observed within both our ambient and nutrient replete experimental treatments (Figs. 4 & 6), with overall treatment effects being of a similar magnitude within the higher temperature lower buffer capacity waters irrespective of nutrient condition (Fig. 6). Although we cannot fully discount a potential direct influence of temperature on the observed differential responses (Fig. 7), we argue that any such influence would have to be through an unknown (eco-) physiological mechanism rather than simply being an artefact of experimental duration.

Specifically, maximum net growth rates might be expected to be around 2 to 3-fold higher in the warmest compared to the coldest waters sampled (Eppley, 1972). Consistent with such expectation, maximum Chl-normalised photosynthetic rates were around 2 to 3-fold higher (Fig. 7) in the lower latitude experiments, as were net growth rates within our nutrient replete experimental treatments ($0.19\text{--}0.27\text{ d}^{-1}$ for $\text{SST} < 3^{\circ}\text{C}$ versus $0.28\text{--}0.68\text{ d}^{-1}$ for $\text{SST} > 12^{\circ}\text{C}$). However, CCS responses in the high latitude experiments remained insignificant, despite a subset of these being up to twice the overall experimental duration (Fig. 2 h, i, Table 1) and 4 times longer than the 2 day time point where MNTes were typically observed within the mid-latitude experiments (Fig. 2).

Although we cannot unequivocally relate causation to correlation, we argue that the association of the strongest MNTes with the lowest buffer capacity waters (Fig. 7) is consistent with theoretical expectations and previous arguments (Flynn *et al.* 2012; Richier *et al.* 2014). Specifically, the magnitude of natural CCS variability encountered by an aquatic organism is a complex function of external forcing (Hofmann *et al.*, 2011), buffering capacity (Hofmann *et al.* 2010; Glas *et al.*, 2012), behaviour (Lewis *et al.*, 2013), cell morphology (Flynn *et al.*, 2012; Hurd *et al.*, 2011), metabolic rate (Flynn *et al.*, 2012; Chrachri *et al.* 2018), and diffusional transport constraints (Glas *et al.*, 2012). All of these factors may interact (Flynn *et al.*, 2012; Richier *et al.*, 2014; Hofmann *et al.*, 2011; Glas *et al.*, 2012) across a broad range of temporal (from hours to days; Hofmann *et al.*, 2011) and spatial (from single organism to ecosystem; Hendrick *et al.*, 2015) scales.

At cellular scales, the microenvironment at the vicinity of the cell, or diffusive boundary layer (DBL), decouples chemical concentrations at the cell surface from those within the surrounding seawater (Wolf-Gladrow *et al.*, 1999; Zeebe *et al.*, 2003; Chrachri *et al.*, 2018), potentially mediating physiological susceptibility to CCS variability (Flynn *et al.*, 2012; Glas *et al.*, 2012; Hurd *et al.*, 2011). Indeed, feedbacks between metabolic processes

(photosynthesis, respiration, calcification) and subsequent CCS variability at the cell surface is highly dependent on the thickness of the DBL (Flynn *et al.*, 2012). Moreover, the thickness of the DBL is itself a function of both cell morphology/cell size (Flynn *et al.*, 2012; Finkel *et al.*, 2010) and ambient seawater flow regime (Glas *et al.*, 2012; Hurd *et al.*, 2011). Consequently, large-celled phytoplankton with thicker DBLs would be expected to experience higher natural CCS variability at the cell surface and hence have a higher inherent tolerance to external CCS forcing than smaller cells (Flynn *et al.*, 2012; Richier *et al.*, 2014).

The observed differential sensitivity of phytoplankton communities to imposed CCS variability within our combined data set (Figs. 3, 4 and 7) is thus consistent with such theoretical considerations (Flynn *et al.*, 2012). Specifically, enhanced susceptibility to rapid CCS changes for natural communities sampled under high buffer capacity conditions may reflect a lower tolerance to external changes in CCS under conditions where natural variability both within bulk seawater and the DBL is lower (Flynn *et al.*, 2012). It is therefore logical to expect that this mechanism would be amplified for smaller cells with thinner DBLs, where the influence of bulk seawater buffering capacity on cell surface buffering should be greatest (Flynn *et al.*, 2012; Richier *et al.*, 2014) (Figs. 4 and 7).

Given the short timescale of the anthropogenic perturbation compared to phytoplankton generation and hence evolutionary timescales (Lohbeck *et al.*, 2012; Schaum *et al.*, 2013, 2016), let alone that of short-term experimental manipulations (Joint *et al.*, 2011), the implications of the proposed mechanisms in the context of future OA remain difficult to specify. The most marked responses that we observed typically occurred over the shortest timescales resolved (2 days) (Richier *et al.*, 2014), with less pronounced differences observable over timescales ≥ 72 h (Fig. 2) when, in some cases, in the absence of additional nutrient enrichment, nutrient exhaustion may have driven the system to a similar state across all treatments (Richier *et al.*, 2014). However, we suggest that the observed dominance of

short response timescales could also reflect subsequent rapid acclimation of the measured phytoplankton populations following an initial stress response caused by the experimental manipulation forcing the small cell sized sub-population outside of their extant acclimative tolerance range.

In addition to our observed short timescale responses not being simply scalable to longer timescales, our results also do not preclude the potential importance of other drivers of interactions between phytoplankton and the CCS, either within experimental studies or under altered future conditions (Riebesell & Tortell, 2011). For example, elevated $p\text{CO}_2$ may also directly facilitate enhanced growth rates, in particular for larger celled phytoplankton (Riebesell & Tortell, 2011; Wu *et al.*, 2011). Minor positive treatment effects in our lower latitude experiments (Fig. 3) would be consistent with such a mechanism, although these observations were not typically significant.

Our results suggest that both short- and long-term experiments (Tatters *et al.*, 2013) investigating the impact of OA may need careful interpretation, as any extant organism lacking in acclimative tolerance to rapid CCS changes might be disadvantaged and hence selected against in the early stages of any CCS manipulation experiment. Although initial community size structure was not a significant predictor of the differential responses (Fig. 7) (Richier *et al.*, 2014), both community composition and the history of prior environmental fluctuations, as mediated by buffer capacity, may thus influence the outcome of experiments over a range of timescales. More broadly, these also influence the selective and evolutionary outcomes of interactions between phytoplankton communities and CCS forcing (Schaum *et al.*, 2016; Flynn *et al.*, 2015; Li *et al.*, 2016).

Oceanic uptake of anthropogenic CO_2 will continue to decrease the CCS buffer capacity in the future (Eggleston *et al.*, 2010; Schaum *et al.*, 2016). Spatial gradients in buffer capacity will also decrease as buffering approaches a minimum where dissolved inorganic

carbon (DIC) and total alkalinity (TA) converge (Fig. 2a) (Egleston *et al.*, 2010). Although our experiments covered a significant range of extant buffer capacity variability in the oceans (Fig. 3a), extension to lower latitude, higher buffer capacity systems would be desirable in future studies. Indeed, low latitude oligotrophic waters with high buffering capacity will experience the greatest absolute changes in the future (Fig. 3a), with up to 22% decreases in resistance to $[H^+]$ variation (Egleston *et al.*, 2010) and corresponding increases in the degree of CCS variability.

In contrast, cold DIC-rich high latitude systems such as we sampled in the Southern Ocean, high latitude North Atlantic and Arctic will be subject to lower decreases, with buffer factors potentially approaching theoretical minima around the end of this century (Fig. 3a) (Orr *et al.*, 2005). Relative changes in the degree of near cell surface CCS variability (Egleston *et al.*, 2010; Flynn *et al.*, 2012; Chrachri *et al.*, 2018) will be larger in mid-latitude temperate systems, but largest in the potentially expanding (Sarmiento *et al.*, 2004; Polovina *et al.*, 2008) low latitude oligotrophic systems. These environments, where extant phytoplankton communities are typically dominated by small celled taxa (Finkel *et al.*, 2010), might be expected to display the lowest inherent acclimative tolerance to CCS variability. Increased $[H^+]$ variability may therefore have the greatest potential to drive adaptive responses of microbial communities (Flynn *et al.*, 2012; Lewis *et al.*, 2013), through a combination of selection or evolution (Schaum *et al.*, 2016), in such low-latitude systems.

Geographically related sensitivities of upper-ocean phytoplankton communities to imposed rapid changes in the CCS (Fig. 2) cautions against simple extrapolation of single or geographically limited experimental results (Joint *et al.*, 2011). Regional environmental variability, including the potential role of decreased seawater buffer capacity and any associated ecosystem feedbacks, needs to be considered alongside a taxonomic, functional

group and evolutionary perspective (Collins *et al.*, 2014; Schaum *et al.*, 2013, 2016; Flynn *et al.*, 2015).

The overall consequences of any buffer capacity and cell size related acclimative tolerances to CCS variability (Figs. 3, 4 and 7) for marine ecosystems and subsequent perturbations to biogeochemical cycles will likely depend on the magnitude of the metabolic costs associated with adaptation to a more variable environment. It is plausible that CCS fluctuations at the cell surface, as a function of cell size (Flynn *et al.*, 2012), location (Hofmann *et al.*, 2011) and altered forcing (Egleston *et al.*, 2010), may influence selection (Schaum *et al.*, 2016; Li *et al.*, 2016; Gaitán-Espitia *et al.*, 2017) and contribute to shifts in phytoplankton community structure (Finkel *et al.*, 2010). For example, energetic costs incurred by organisms requiring higher active H⁺ and/or HCO₃⁻ transport for cellular homeostasis purposes (Flynn *et al.*, 2012; Taylor *et al.*, 2012), may trade-off against the consequences of poorer cellular acid-base regulation or the requirement to be smaller (Schlüter *et al.*, 2014). Despite any remaining ecophysiological uncertainties, our study highlights how organism and ecosystem responses to OA need to be considered not only in the context of changes to the mean CCS state, but also in relation to the magnitude of CCS variability experienced by organisms at cellular scales (Flynn *et al.*, 2012; Schaum *et al.*, 2016; Chrachri *et al.*, 2018). We suggest that these factors may be fundamentally linked to the regionally variable buffering characteristics of oceanic waters.

Acknowledgments

This work was funded under the UK Ocean Acidification (UKOA) programme via Natural Environment Research Council grants NE/H017348/1 to T. Tyrrell, E. P. Achterberg and C. M. Moore; NE/H017097/1 to A. J. Poulton; NE/H017062/1 to D. J. Suggett and a studentship to M. P. Humphreys. Contributions to D. J. Suggett were also supported through

579 an Australian Research Council Future Fellowship (FT130100202). We thank C.
580 Dumousseaud, M. Ribas Ribas and E. Tynan for processing carbonate chemistry analyses and
581 M. Stinchcombe for nutrient data. We are also grateful to A. Yool for the model output and to
582 T. Bibby and D. Allemand for discussions and/or comments on the manuscript.

References

- Bach, L. T, Riebesell, U., Gutowska, M. A., Federwisch, L., & Schulz, K. G. (2015). A unifying concept of coccolithophore sensitivity to changing carbonate chemistry embedded in an ecological framework. *Progress in Oceanography*, 135, 125-138.
- Behrenfeld, M. J., & Falkowski, P. G. (1997) Photosynthetic rates derived from satellite-based chlorophyll concentration. *Limnology and Oceanography*, 42, 1-20.
- Boyd, P. W., Strzepek, R., Fu, F. X., & Hutchins, D. A. (2010) Environmental control of open-ocean phytoplankton groups: now and in the future. *Limnology and Oceanography*, 55, 1353–1376.
- Boyd, P. W. (2011) Beyond ocean acidification. *Nature Geoscience*. 4, 273–274.
- Boyd, P. W., Lennartz, S. T., Glover, D. M., & Doney, S. C. (2015) Biological ramifications of climate-change mediated oceanic multi-stressors. *Nature Climate Change*, 5, 71-79.
- Boyd, P. W., Cornwall, C. E., Davison, A., Doney, S. C., Fourquez, M., Hurd, C. L., Lima, I. D., & McMin, A. (2016) Biological response to environmental heterogeneity under future ocean conditions. *Global Change Biology*, 22, 2633-2650.
- Chrachri, A., Hopkinson, B. M., Flynn, K., Brownlee C., & Wheeler G. L. (2018) Dynamic changes in carbonate chemistry in the microenvironment around single marine phytoplankton cells. *Nature Communications*, doi:10.1038/s41467-017-02426-y.
- Collins, S., Rost, R., & Rynearson, T. A. (2014) Evolutionary potential of marine phytoplankton under ocean acidification. *Evolutionary Applications*, 7, 140-155.
- Cullen, J., & Davis, R. (2003) The blank can make a big difference in oceanographic measurements. *Limnology and Oceanography Bulletin*, 12, 29-35.

607 Denman, K., Christian, J. R., Steiner, N., Pörtner, H. -O., & Nojiri, Y. (2011) Potential
608 impacts of future ocean acidification on marine ecosystems and fisheries: current
609 knowledge and recommendations for future research. *ICES Journal of Marine Science*,
610 68, 1019-1029.

611 Dickson, A. G., & Millero, F. J. (1987) A comparison of the equilibrium constants for
612 the dissociation of carbonic acid in seawater media. *Deep-Sea Research Part II*, 34,
613 1733–1743.

614 Doney, S. C., Fabry, V. J., Feely, R. A., & Kleypas, J. A. (2009) Ocean Acidification:
615 The Other CO₂ Problem. *Annual Review of Marine Science*, 1, 169-192.

616 Dutkeiwicz, S., Morris, J. J., Follows, M. J., Scott, J., Levitan, O., Dyhrman, S. T., &
617 Berman-Frank, I. (2015) Impact of ocean acidification on the structure of future
618 phytoplankton communities. *Nature Climate Change*, 5, 1002-1006.

619 Egleston, E. S., Sabine, C. L., Morel, F. M. M. (2010) Revelle revisited: Buffer
620 factors that quantify the response of ocean chemistry to changes in DIC and alkalinity.
621 *Global Biogeochemical Cycles*, 24, GB1002.

622 Eppley, R. W. (1972) Temperature and phytoplankton growth in the sea. *Fishery*
623 *Bulletin*, 70, 1063-1085.

624 Finkel, Z. V., Beardall, J., Flynn, K. J., et al. (2010) Phytoplankton in a changing
625 world: cell size and elemental stoichiometry. *Journal of Plankton Research*, 32, 119-
626 137.

627 Flynn, K. J., Blackford, J. C., Baird, M. E., et al. (2012) Changes in pH at the exterior
628 surface of plankton with ocean acidification. *Nature Climate Change*, 2, 510-513.

629 Flynn, K. J., Clark, D. R., Mitra, A., et al. (2015) Ocean acidification with
630 (de)eutrophication will alter future phytoplankton growth and succession.
631 *Proceedings of the Royal Society of London B*, **282**, 20142604.

632 Frankignoulle, M. A. (1994) Complete set of buffer factors for acid/base CO₂ system
633 in seawater. *Journal of Marine Systems*, **5**, 111-118.

634 Gaitán-Espitia, J. D., Marshall, D., Dupont, S., Bacigalupe, L.D., Bodrossy, L., &
635 Hobday, A. J. (2017) Geographical gradients in selection can reveal genetic
636 constraints for evolutionary responses to ocean acidification. *Biology Letters*, **13**,
637 20160784. <http://dx.doi.org/10.1098/rsbl.2016.0784>.

638 Glas, M. S., Fabricius, K. E., de Beer, D., & Uthicke, S. (2012) The O₂, pH and Ca²⁺
639 Microenvironment of Benthic Foraminifera in a High CO₂ World. *PLoS ONE*, **7**,
640 e50010.

641 Hendricks, I. E., Duarte, C. M., Olsen, Y. S., et al. (2015) Biological mechanisms
642 supporting adaptation to ocean acidification in coastal ecosystems. *Estuarine, Coastal*
643 *and Shelf Science*, **152**, A1-A8.

644 Hofmann, G. E., Smith, J. E., Johnson, K. S., et al. (2011) High-Frequency Dynamics
645 of Ocean pH: A Multi-Ecosystem Comparison. *PloS ONE*, **6**, e28983.

646 Hofmann, A. F., Middelburg, J. J., Soetaert, K., Wolf-Gladrow, D. A., & Meysman,
647 F. J. R. (2010) Proton cycling, buffering, and reaction stoichiometry in natural waters.
648 *Marine Chemistry*, **121**, 246-255.

649 Hoppe, C. J., Hassler, C. S., Payne, C. D., et al. (2013) Iron limitation modulates
650 ocean acidification effects on southern ocean phytoplankton communities. *PLoS ONE*,
651 **8**, e79890.

652 Humphreys, M. P. (2017) Climate sensitivity and the rate of ocean acidification:
653 future impacts, and implications for experimental design. *ICES Journal of Marine*
654 *Science*, 74, 934-940.

655 Hurd, C. L., Cornwall, C. E., Currie, K., et al. (2011) Metabolically induced pH
656 fluctuations by some coastal calcifiers exceed projected 22nd century ocean
657 acidification: a mechanism for differential susceptibility? *Global Change Biology*, 17,
658 3254-3262.

659 Joint, I., Doney, S. C., & Karl, D. M. (2011) Will ocean acidification affect marine
660 microbes? *ISME Journal*, 5, 1-7.

661 Key, R. M., Kozyr, A., Sabine, C. L., et al. (2004) A global ocean carbon
662 climatology: Results from Global Data Analysis Project (GLODAP). *Global*
663 *Biogeochemical Cycle*, 18, GB4031.

664 Kolber, Z. S., Prasil, O., & Falkowski, P. G. (1998) Measurements of variable
665 chlorophyll fluorescence using fast repetition rate techniques: defining methodology
666 and experimental protocols. *BBA- Bioenergetics*, 1367, 88-106.

667 Kroeker, K. J., Kordas, R. L., Crim, R., et al. (2013) Impacts of ocean acidification on
668 marine organisms: quantifying sensitivities and interaction with warming. *Global*
669 *Change Biology*, 19, 1884-1896.

670 Lewis, E., & Wallace, D. W. R. (1998) Program developed for CO₂ system calculations.
671 ORNL/CDIAC-105. *Carbon Dioxide Information Analysis Center* (Oak Ridge National
672 Laboratory, US Department of Energy, Oak Ridge, Tennessee).

673 Lewis, C. N., Brown, K. A., Edwards, L. A., Cooper, G., & Findlay, H. S. (2013)
674 Sensitivity to ocean acidification parallels natural pCO₂ gradients experienced by

675 Arctic copepods under winter sea ice. *Proceedings of the National Academy of*
676 *Sciences USA*, 110, E4960-E4967.

677 Li, W., Gao, K., & Beardall, J. (2012) Interactive effects of OA and N-limitation on
678 the diatom *Phaeodactylum tricornutum*. *PLOS one* 7, e51590.

679 Li, F., Wu, Y., Hutchins, D. A., Fu, F., Gao, K. (2016) Physiological responses of
680 coastal and oceanic diatoms to diurnal fluctuations in seawater carbonate chemistry
681 under two CO₂ concentrations. *Biogeosciences*. 13, 6247-6259.

682 Lohbeck, K. T., Riebesell, U., & Reusch, T. H. (2012) Adaptive evolution of a key
683 phytoplankton species to ocean acidification. *Nature Geoscience*, 5, 346-351.

684 Mehrbach, C., Culberson, C. H., Hawley, J. E., & Pytkowicz, R. M. (1973)
685 Measurement of apparent dissociation-constants of carbonic-acid in seawater at
686 atmospheric pressure. *Limnology and Oceanography*, 18, 897-907.

687 Muller, M. N., Trull, T. W., & Hallegraeff, G. M. (2017) Independence of nutrient
688 limitation and carbon dioxide impacts on the Southern Ocean coccolithophore
689 *Emiliana huxleyi*. *The ISME Journal*, 11-1777-1787.

690 Orr, J. C., Fabry, V. J., Aumont, O., et al. (2005) Anthropogenic ocean acidification
691 over the twenty-first century and its impact on calcifying organisms. *Nature*, 437, 681-
692 686.

693 Pierrot, D., Lewis, E., & Wallace, D. W. R. (2006) MS Excel Program Developed for
694 CO₂ System Calculations, ORNL/CDIAC-105. *Carbon Dioxide Information Analysis*
695 *Center* (Oak Ridge National Laboratory, US Department of Energy, Oak Ridge,
696 Tennessee).

697 Polovina, J. J., Howell, E. A., & Abecassis, M. (2008) Ocean's least productive waters
698 are expanding. *Geophysical Research Letters*, 35, L03618.

699 Poulton, A. J., Daniels, C. J., Esposito, M et al. (2016) Production of dissolved
700 organic carbon by Arctic plankton communities: Responses to elevated carbon
701 dioxide and the availability of light and nutrients. *Deep-Sea Research Part II*, 127, 60-
702 74.

703 Raimbault, P., Diaz, F., Pouvesle, W., & Boudjellal, B. (1999) Simultaneous
704 determination of particulate organic carbon, nitrogen and phosphorus collected on
705 filters, using a semi-automatic wet-oxidation method. *Marine Ecology Progress Series*,
706 180, 289–295.

707 Reusch, T. B. H., & Boyd, P. W. (2013) Experimental evolution meets marine
708 phytoplankton. *Evolution*, 67, 1849-1859.

709 Richier, S., Achterberg, E. P., Dumousseaud, C., et al. (2014) Phytoplankton
710 responses and associated carbon cycling during shipboard carbonate chemistry
711 manipulation experiments conducted around Northwest European shelf seas.
712 *Biogeosciences*, 11, 4733-4752.

713 Riebesell, U., & Tortell, P. D. (2011) Effects of ocean acidification on pelagic
714 organisms and ecosystems. *Ocean Acidification* (Univ of Oxford Press), pp 99-121.

715 Riebesell, U., Bach, L. T., Bellerby, R. G. J., Bermudez, Monsalve, J. R.,
716 Boxhammer, T., et al. (2017) Competitive fitness of a predominant pelagic calcifier
717 impaired by ocean acidification. *Nature Geoscience*, 10, 19-23.

718 Royal Society (2005). Ocean Acidification Due to Increasing Atmospheric Carbon
719 Dioxide, 60, Policy Document 12/05, The Royal Society, London.

720 Sarmiento, J. L., Slater, R., Barber, R., et al. (2004) Response of ocean ecosystems to
721 climate warming. *Global Biogeochemical Cycle*, 18, GB3003.

722 Schaum, C. E., Rost, B., Millar, A. J., & Collins, S. (2013) Variation in plastic
723 responses of a globally distributed picoplankton species to ocean acidification. *Nature*
724 *Climate Change*, 3, 298-302.

725 Schaum, C. E., Rost, B., & Collins, S. (2016) Environmental stability affects
726 phenotypic evolution in a globally distributed marine picoplankton. *ISME Journal*, 10,
727 75-84.

728 Schlüter, L., Lohbeck, K. T., Gutowska, M. A., et al. (2014) Adaptation of a globally
729 important coccolithophore to ocean warming. *Nature Climate Change*, 4, 1024-1030.

730 Sunda, W. G., Price, N. M., & Morel, F. M. M. (2005) Trace metal ion buffers and their
731 use in culture studies. *Algal Culturing Techniques*, ed. Anderson RA (Elsevier), pp 35-
732 65.

733 Sundquist, E. T., Plummer, L. N., & Wigley, T. M. L. (1979) Carbon-dioxide in the
734 ocean surface-homogeneous buffer factor. *Science*, 204, 1203-1205.

735 Tarling, G. A., Peck, V., Ward, P., et al. (2016) Effects of acute ocean acidification on
736 spatially-diverse polar pelagic foodwebs: Insights from on-deck microcosms. *Deep-*
737 *Sea Research II*, 127, 75-92.

738 Tatters, A. O., Roleda, M. Y., Schnetzer, A., et al. (2013) Short- and long-term
739 conditioning of a temperate marine diatom community to acidification and warming.
740 *Philosophical Transactions of the Royal Society B-Biological Sciences*, 368, 1627.

741 Tatters, A. O., Schnetzer, A., Fu, F., et al. (2013) Short-versus long-term responses to
742 changing CO₂ in a coastal dinoflagellate bloom: Implications for interspecific
743 competitive interactions and community structure. *Evolution*, 67, 1879-1891.

744 Taylor, A. R., Brownlee, C., & Wheeler, G. L. (2012) Proton channels in algae:
745 reasons to be excited. *Trends in Plant Science*, 17, 675-684.

- Trimborn, S., Brenneis, T., Hoppe, C. J. M., et al. (2017) Iron sources alter the response of Southern Ocean phytoplankton to ocean acidification. *Marine Ecology Progress Series*. 578, 35-50.
- Tynan, E., Clarke, J. S., Humphreys, M. P., et al. (2016) Physical and biogeochemical controls on the variability in surface pH and calcium carbonate saturation states in the Atlantic sectors of the Arctic and Southern Oceans. *Deep Sea Research Part II*, 127, 7-27.
- Welschmeyer, N. A. (1994) Fluorometric analysis of chlorophyll a in the presence of chlorophyll b and pheopigments. *Limnology and Oceanography*, 39, 1985-1992.
- Wolf-Gladrow, D. A., Bijma, J., & Zeebe, R. E. (1999) Model simulation of the carbonate chemistry in the microenvironment of symbiont bearing foraminifera. *Marine Chemistry*, 64, 181-198.
- Wu, Y., Campbell, D. A., Irwin, A. J., Suggett, D. J., & Finkel, Z.V. (2014) Ocean acidification enhances the growth rate of larger diatoms. *Limnology and Oceanography*, 59, 1027-1034.
- Zeebe, R. E., Wolf-Gladrow, D. A., Bijma, J., & Hornisch, B. (2003) Vital effects in foraminifera do not compromise the use of $\delta^{11}\text{B}$ as a paleo-pH indicator: Evidence from modelling. *Paleoceanography*, 18, 1043.
- Yool, A., Popova, E. E., Coward, A. C., Bernie, D., & Anderson, T. R. (2013) Climate change and ocean acidification impacts on lower trophic levels and the export of organic carbon to the deep ocean. *Biogeosciences*, 10, 5831-5854.

Author contributions

C.M.M, E.P.A, A.J.P., T.T., and D.J.S. designed the research. C.M.M., S.R., A.J.P., T.T., and D.J.S. conceived and designed the experiments. S.R., C.M.M., E.P.A., A.J.P., T.T., and D.J.S. performed the experiments. S.R. and C.M.M analysed and interpreted the data. S.R. and C.M.M wrote the manuscript. All authors contributed to discussions of the results and subsequent editing of the paper.